Journal of Systems Engineering and Electronics
Vol. 30, No. 5, October 2019, pp.985 – 994

Dual-quaternion-based modeling and control for motion tracking of a tumbling target

PENG Xuan[1,*], SHI Xiaoping[1], and GONG Yupeng[2]

1. Control and Simulation Center, Harbin Institute of Technology, Harbin 150001, China;
2. Research Center of Satellite Technology, Harbin Institute of Technology, Harbin 150001, China

Abstract: This paper investigates the problem of controlling a chasing spacecraft (chaser) to track and rendezvous with an uncontrolled target. Based on the actual situation, the torque-free motion of an axisymmetric prolate rigid body is employed to represent the short-term attitude motion of the tumbling target. By taking advantage of the dual quaternion's compact and efficient description of the general rigid motion, the coupled and integrated model of the 6-degree-of-freedom (6-DOF) relative motion between the chaser and the tumbling target is derived in the chaser's body fixed frame after taking full consideration of coordinate transformation. Based on the logarithm of dual quaternion, a sliding mode control (SMC) law based on the exponential reaching law and the continuous relay function is brought forward to address the problem of synchronization control of the 6-DOF relative motion. Simulation results illustrate the effectiveness of the proposed method.

Keywords: tumbling target, dual-quaternion, coupled dynamics, relative motion.

DOI: 10.21629/JSEE.2019.05.15

1. Introduction

On-orbit service is helpful to remove space debris, prolong orbital lifetime and enhance performance of targets, which is significant for sustainable development of the aerospace industry [1,2]. As for on-orbit service missions, many targets, such as dysfunctional or spent satellites, have lost the ability of attitude adjustment. Under influences of perturbation torques and residual angular momentum before failure, they usually have complex rotational motion, such as spin or tumbling [3,4]. To track and rendezvous with these unstable targets, relative attitude and position should be simultaneously controlled with high precision, which requires an accurate model of the 6-degree-of-freedom (6-DOF) relative motion. The conventional model neglects strong coupling between rotation and translation, and is no longer applicable in spacecraft proximity missions nowadays [5 – 7]. In recent years, the 6-DOF coupled model has been actively studied [8]. In [9 – 13], coupled dynamics of relative motion between the tumbling target and the chaser is derived by two steps. First, the rotation and translation are modeled separately. Usually, the relative rotation model is established in body fixed frame by quaternion or modified Rodrigues parameters. Moreover, the relative translation model is established in the target's orbit frame or the chaser's line-of-sight frame by the position vector. Then, the two parts are incorporated into one united framework based on kinematic and dynamic couplings. Mixed calculation between different coordinates and mathematical tools increases complexity of the model and is inefficient. Besides, given that the couplings between relative attitude and position are intricate, this method cannot guarantee to take all coupling terms into consideration, let alone establish the accurate model of the 6-DOF relative motion.

In contrast to this two-part modeling method, a dual quaternion enables the model of 6-DOF relative motion to be integrated, which is a more effective approach to deal with the coupled modeling. Composed of real and dual parts, a dual quaternion could describe the attitude and position simultaneously with only eight parameters. Therefore, couplings between rotation and translation are automatically contained within the dual-quaternion-based model, which also has advantages of non-singularity, compactness, high computation efficiency and explicit physical meaning [14 – 17]. Brodsky et al. [18] first established coupled dynamics of a single rigid body by dual quaternion. Wang et al. [19] first derived the dual-quaternion-based coupled dynamics of the 6-DOF relative motion between two spacecraft and proposed a terminal sliding mode pose tracking control law. Based on the model given in [19], various control laws for relative position and attitude tracking were further explored and designed in [20 – 25]. However, the model of relative motion presented in [19] was

Manuscript received February 18, 2019.
*Corresponding author.
This work was supported by the National Science Foundation of China (61427809).

developed under the assumption that the target is stable in its orbit and the target body fixed frame is always aligned with the target orbital frame, which is obviously invalid in the case of the tumbling target.

Thus far, there exist few research results about dual-quaternion-based modeling of the relative motion between the chaser and a tumbling target, which is exactly what this paper focuses on. Unlike [10,26,27], where the tumbling target was assumed to rotate at an arbitrary constant angular velocity, in this paper the attitude motion of the target is derived based on the attitude dynamics, which can better represent its real motion state. Fully considering transformation among different coordinates, all linear and angular velocities, radius vectors and so on are converted to the chaser's body fixed frame, then the integrated model based on dual quaternion that describes the 6-DOF motion of the chaser's body fixed frame relative to the target's body fixed frame is derived in detail. Finally, a sliding mode control (SMC) controller with an exponential reaching law and a continuous relay function is designed and then simulated. The effectiveness of the proposed approach is verified by simulation results.

2. Preliminaries

In this section, some basic concepts and operation rules of quaternion and dual quaternion are summarized to provide essential foundations for the development of main results presented. More details involving these can be found in [28–31].

2.1 Quaternion

Invented by Hamilton, a quaternion $\boldsymbol{q}$ is defined as a complex number

$$\boldsymbol{q} = q_0 + q_1\mathrm{i} + q_2\mathrm{j} + q_3\mathrm{k} \tag{1}$$

formed from imaginary basis units $(1, \mathrm{i}, \mathrm{j}, \mathrm{k})$ by means of real numbers q_0, q_1, q_2 and q_3, where $\mathrm{i}^2 = \mathrm{j}^2 = \mathrm{k}^2 = \mathrm{ijk} = -1$. q_0 is the scalar part and $q_1\mathrm{i} + q_2\mathrm{j} + q_3\mathrm{k}$ is the vector part.

Note that scalars and 3D vectors can be equivalently viewed as corresponding quaternions with zero vector and zero scalar parts and vice versa.

For computational convenience, in what follows, the matrix (4D vector) form of a quaternion is used, which is defined as

$$\boldsymbol{q} = [q_0 \quad \boldsymbol{q}_v]^{\mathrm{T}}, \quad \boldsymbol{q}_v = [q_1 \quad q_2 \quad q_3]^{\mathrm{T}}. \tag{2}$$

The identity and zero elements of quaternions are defined as $\mathbf{1} = [1 \quad \mathbf{0}_v]^{\mathrm{T}}$, $\mathbf{0} = [0 \quad \mathbf{0}_v]^{\mathrm{T}}$ with $\mathbf{0} = [0 \quad 0 \quad 0]^{\mathrm{T}}$.

Consider two quaternions in matrix form, $\boldsymbol{a} = [a_0 \quad \boldsymbol{a}_v^{\mathrm{T}}]^{\mathrm{T}}$, $\boldsymbol{b} = [b_0 \quad \boldsymbol{b}_v^{\mathrm{T}}]^{\mathrm{T}}$, and some operations on quaternion are given as follows:

$$\begin{cases} \text{Conjugation: } \boldsymbol{a}^* = [a_0 \quad -\boldsymbol{a}_v^{\mathrm{T}}]^{\mathrm{T}} \\ \text{Multiplication: } \boldsymbol{a} \circ \boldsymbol{b} = \begin{bmatrix} a_0 b_0 - \boldsymbol{a}_v \cdot \boldsymbol{b}_v \\ a_0 \boldsymbol{b}_v + b_0 \boldsymbol{a}_v + \boldsymbol{a}_v \times \boldsymbol{b}_v \end{bmatrix} \\ \text{Cross product:} \\ \qquad \boldsymbol{a} \times \boldsymbol{b} = \dfrac{1}{2}(\boldsymbol{a} \circ \boldsymbol{b} - \boldsymbol{b} \circ \boldsymbol{a}) = \begin{bmatrix} 0 \\ \boldsymbol{a}_v \times \boldsymbol{b}_v \end{bmatrix} \\ \text{Dot product:} \\ \qquad \boldsymbol{a} \cdot \boldsymbol{b} = \dfrac{1}{2}(\boldsymbol{a} \circ \boldsymbol{b}^* + \boldsymbol{b} \circ \boldsymbol{a}^*) = \begin{bmatrix} a_0 b_0 + \boldsymbol{a}_v \cdot \boldsymbol{b}_v \\ 0 \end{bmatrix} \\ \text{Norm: } N^2(\boldsymbol{a}) = \boldsymbol{a} \circ \boldsymbol{a}^* = \boldsymbol{a}^* \circ \boldsymbol{a} \end{cases}. \tag{3}$$

The quaternion multiplication can be written in a compact form as

$$\boldsymbol{a} \circ \boldsymbol{b} = \boldsymbol{a}^+ \boldsymbol{b} = \boldsymbol{b}^- \boldsymbol{a}. \tag{4}$$

$\boldsymbol{a}^+$ and $\boldsymbol{b}^-$ are 4×4 matrices, which are given as

$$\begin{aligned} \boldsymbol{a}^+ &= \begin{bmatrix} a_0 & -\boldsymbol{a}_v^{\mathrm{T}} \\ \boldsymbol{a}_v & a_0 \boldsymbol{I} + \boldsymbol{S}(\boldsymbol{a}_v) \end{bmatrix} \\ \boldsymbol{b}^- &= \begin{bmatrix} b_0 & -\boldsymbol{b}_v^{\mathrm{T}} \\ \boldsymbol{b}_v & b_0 \boldsymbol{I} - \boldsymbol{S}(\boldsymbol{b}_v) \end{bmatrix} \end{aligned} \tag{5}$$

where $\boldsymbol{I}$ is a 3×3 unit matrix, $\boldsymbol{S}(\boldsymbol{a}_v)$ is defined as

$$\boldsymbol{S}(\boldsymbol{a}_v) = \begin{bmatrix} 0 & -a_3 & a_2 \\ a_3 & 0 & -a_1 \\ -a_2 & a_1 & 0 \end{bmatrix}. \tag{6}$$

Applying (4) to multiplication of three quaternions $\boldsymbol{a}$, $\boldsymbol{b}$ and $\boldsymbol{c}$, there is

$$\boldsymbol{a} \circ \boldsymbol{b} \circ \boldsymbol{c} = \boldsymbol{a}^+ \boldsymbol{c}^- \boldsymbol{b}. \tag{7}$$

A unit quaternion satisfies $N^2(\boldsymbol{q}) = \mathbf{1}$. It can be used to represent arbitrary rotation. Supposing a frame A rotates about a unit axis $\boldsymbol{u}$ with an angle Φ and becomes the frame B, this rotation can be described by the unit quaternion $\boldsymbol{q} = [\cos(\Phi/2) \quad \sin(\Phi/2)\boldsymbol{u}^{\mathrm{T}}]^{\mathrm{T}}$. The expressions of a fixed vector $\boldsymbol{r}$ in frames A and B are related by

$$\boldsymbol{r}^b = \boldsymbol{q}^* \circ \boldsymbol{r}^a \circ \boldsymbol{q} = \begin{bmatrix} 1 & 0^{\mathrm{T}} \\ 0 & \boldsymbol{C}(\boldsymbol{q}) \end{bmatrix} \begin{bmatrix} 0 \\ \boldsymbol{r}^a \end{bmatrix} \tag{8}$$

where $\boldsymbol{C}(\boldsymbol{q}) = q_0^2 \boldsymbol{I} - 2q_0 \boldsymbol{S}(\boldsymbol{q}_v) + \boldsymbol{S}(\boldsymbol{q}_v)\boldsymbol{S}(\boldsymbol{q}_v)$ is the direction cosine matrix (DCM) of the rotation represented by $\boldsymbol{q}$.

Besides, the logarithm of a unit quaternion $\boldsymbol{q}$ is defined as

$$\ln \boldsymbol{q} = \frac{\Phi}{2}\boldsymbol{u} = \frac{\arccos q_0}{\sqrt{1 - q_0^2}} \boldsymbol{q}_v = \frac{\Phi}{2} \overline{\boldsymbol{q}}_v \tag{9}$$

where $\Phi = 2 \arccos q_0$, $\overline{\boldsymbol{q}}_v = \boldsymbol{q}_v / \sqrt{1 - q_0^2}$.

2.2 Dual number and dual vector

Introduced by Clifford, a dual number $\widehat{a}$ can be defined as an ordered pair combing a real part a and a dual part a':

$$\widehat{a} = a + \varepsilon a' \tag{10}$$

where a and a' are real numbers, ε is the dual unit (operator), which satisfies $\varepsilon^2 = 0$ and $\varepsilon \neq 0$. When applied to a dual number, there is $\varepsilon\widehat{a} = \varepsilon(a + \varepsilon a') = \varepsilon a + \varepsilon^2 a' = \varepsilon a$.

In space geometry, the dual number can be used to represent the relative displacement and orientation between two space lines. That is, a dual angle is defined as

$$\widehat{\theta} = \theta + \varepsilon d \tag{11}$$

where θ is the projected angle between two lines and d is the shortest distance between them, i.e., the length of common perpendicular. For the dual angle θ, we have

$$\begin{aligned} \sin\widehat{\theta} = \sin(\theta + \varepsilon d) = \sin\theta + \varepsilon d\cos\theta \\ \cos\widehat{\theta} = \cos(\theta + \varepsilon d) = \cos\theta - \varepsilon d\cos\theta \end{aligned}. \tag{12}$$

A dual vector is a dual number, whose real part $\boldsymbol{a}$ and dual part $\boldsymbol{a}'$ are both 3D real vectors. A dual vector $\widehat{\boldsymbol{a}}$ is defined as

$$\widehat{\boldsymbol{a}} = \boldsymbol{a} + \varepsilon\boldsymbol{a}'. \tag{13}$$

The unit condition of a dual vector is $N^2(\boldsymbol{a}) = 1$ and $\boldsymbol{a}\cdot\boldsymbol{a}' = 0$. Unit dual vectors can be used to represent space lines. As shown in Fig. 1, a space line passes the point P and its unit direction vector is $\boldsymbol{l}$. It can be described as $\widehat{\boldsymbol{L}} = \boldsymbol{l} + \varepsilon\boldsymbol{m}$ and $\boldsymbol{m}$ is the line moment relative to the origin.

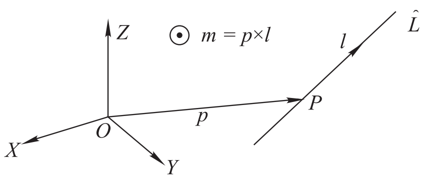

Fig. 1 Space line

A dual vector is termed as a motor if its real part is a free vector which is independent of the reference point and its dual part is a location vector which varies with the choice of reference points. In this sense, the dual velocity vector, dual force vector and dual momentum vector involved in later sections can all be perceived as motors.

2.3 Dual quaternion

A dual quaternion $\widehat{\boldsymbol{q}}$ can be viewed as a dual number with quaternion components:

$$\widehat{\boldsymbol{q}} = \boldsymbol{q} + \varepsilon\boldsymbol{q}' \tag{14}$$

where $\boldsymbol{q} = [q_0 \quad q_1 \quad q_2 \quad q_3]^{\mathrm{T}}$ and $\boldsymbol{q}' = [q_0' \quad q_1' \quad q_2' \quad q_3']^{\mathrm{T}}$ are two quaternions.

Similar to quaternions, for convenience, we also use the vector form of dual quaternions in computation. The vector form of a dual quaternion is defined as a 8D column vector. The vector form of $\widehat{\boldsymbol{q}}$ is defined as

$$\widehat{\boldsymbol{q}} = [q_0 \quad q_1 \quad q_2 \quad q_3 \quad q_0' \quad q_1' \quad q_2' \quad q_3']^{\mathrm{T}}. \tag{15}$$

$\widehat{\boldsymbol{1}} = [\boldsymbol{1} \quad \boldsymbol{0}]^{\mathrm{T}}$ and $\widehat{\boldsymbol{0}} = [\boldsymbol{0} \quad \boldsymbol{0}]^{\mathrm{T}}$ are the identity and zero elements of dual quaternions.

Consider dual quaternions $\widehat{\boldsymbol{q}}_1 = \boldsymbol{q}_1 + \varepsilon\boldsymbol{q}_1'$ and $\widehat{\boldsymbol{q}}_2 = \boldsymbol{q}_2 + \varepsilon\boldsymbol{q}_2'$. Some necessary operations written in the vector form are given as

$$\begin{cases} \text{Conjugate: } \widehat{\boldsymbol{q}}^* = \begin{bmatrix} \boldsymbol{q}^* \\ (\boldsymbol{q}')^* \end{bmatrix} \\ \text{Swap: } \widehat{\boldsymbol{q}}^s = \begin{bmatrix} \boldsymbol{q}' \\ \boldsymbol{q} \end{bmatrix} \\ \text{Multiplication: } \widehat{\boldsymbol{q}}_1 \circ \widehat{\boldsymbol{q}}_2 = \begin{bmatrix} \boldsymbol{q}_1 \circ \boldsymbol{q}_1 \\ \boldsymbol{q}_1 \circ \boldsymbol{q}_2' + \boldsymbol{q}_1' \circ \boldsymbol{q}_2 \end{bmatrix} \\ \text{Circle product: } \widehat{\boldsymbol{q}}_1 \odot \widehat{\boldsymbol{q}}_2 = \begin{bmatrix} \boldsymbol{q}_1 \cdot \boldsymbol{q}_2 \\ \boldsymbol{q}_1' \cdot \boldsymbol{q}_2' \end{bmatrix} \\ \text{Norm: } N^2(\widehat{\boldsymbol{q}}) = \widehat{\boldsymbol{q}} \circ \widehat{\boldsymbol{q}}^* = \widehat{\boldsymbol{q}}^* \circ \widehat{\boldsymbol{q}} \end{cases}. \tag{16}$$

A unit dual quaternion satisfies $N^2(\widehat{\boldsymbol{q}}) = \widehat{\boldsymbol{1}}$. Similar to the way that unit quaternion is used to describe rotation, a unit dual quaternion can be employed to represent any rigid transformations consisting of rotation and translation. In Fig. 2, the general rigid motion between the frame A and the frame B is described by a rotation $\boldsymbol{q}$ followed by a translation $\boldsymbol{t}^b$ (or a translation $\boldsymbol{t}^a$ followed by a rotation $\boldsymbol{q}$), which is equivalent to a rotation about the screw axis $\widehat{\boldsymbol{N}}$ with the angle θ succeeded by a translation $\boldsymbol{d}$ parallel to the axis, namely a screw motion. This frame transformation can be specified by

$$\widehat{\boldsymbol{q}} = \boldsymbol{q} + \varepsilon\boldsymbol{q}' = \boldsymbol{q} + \varepsilon\frac{1}{2}\boldsymbol{q}\circ\boldsymbol{t}^b = \boldsymbol{q} + \varepsilon\frac{1}{2}\boldsymbol{t}^a\circ\boldsymbol{q}. \tag{17}$$

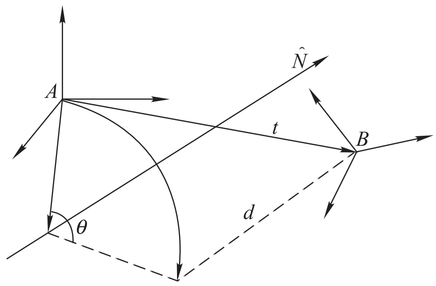

Fig. 2 Transformation of coordinates

Using elements of screw motion, the unit dual quaternion can also be written as

$$\widehat{\boldsymbol{q}} = \cos(\widehat{\theta}/2) + \widehat{\boldsymbol{N}}\sin(\widehat{\theta}/2). \tag{18}$$

The expressions of a fixed dual vector $\widehat{\boldsymbol{r}}$ in coordinates A and B are related by

$$\widehat{\boldsymbol{r}}^b = \widehat{\boldsymbol{q}}^* \circ \widehat{\boldsymbol{r}}^a \circ \widehat{\boldsymbol{q}}. \tag{19}$$

Besides, the logarithm of a unit dual quaternion defined by (17) is given as

$$\ln \widehat{\boldsymbol{q}} = \ln \boldsymbol{q} + \varepsilon \boldsymbol{t}^b/2 = \varPhi \overline{\boldsymbol{q}}_v/2 + \varepsilon \boldsymbol{t}^b/2. \tag{20}$$

Comparing Section 2.1 and Section 2.3, we can see that there are many similarities between quaternion and dual quaternion. In fact, based on the principle of transference formulated by Kotelnikov, dual quaternion completely inherits the properties of quaternion.

2.4 Coordinates

The coordinates used in the following modeling process are given in Fig. 3.

Earth centered inertial frame: denoted as F_I. Its origin is at the center of the earth. The axis x_i points to the vernal equinox, axis y_i points to the North Pole, and axis z_i is given by the right-hand rule.

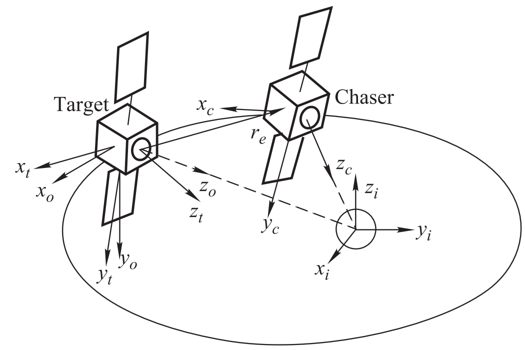

Fig. 3 Coordinates for the relative motion

Body fixed frame: denoted as F_B. Its origin is at the center of mass (c.m.) of the spacecraft and three axes are aligned with principal axes of inertia. Body fixed frames of the chaser and the target are denoted as F_C and F_T, respectively.

Orbit frame: denotes as F_O. This frame is centered at the c.m. of the spacecraft. The axis z_o directs from the spacecraft radially inward, axis y_o is negative normal to the orbit plane, and axis x_o completes the setup.

3. Problem formulation

The problem investigated in this paper is to simultaneously control the relative position and attitude with high precision during the final phrase of approaching a passive tumbling target.

3.1 Attitude motion of the target

The target is assumed to be a rigid body without the control torque. Since spatial disturbances torques are negligible, it is reasonable to represent the target's short-term motion characteristics by the attitude motion in the torque-free state. The target's attitude dynamics is given by Euler's rotational equation

$$\boldsymbol{J}_t \dot{\boldsymbol{\omega}}_t + \boldsymbol{\omega}_t \times (\boldsymbol{J}_t \boldsymbol{\omega}_t) = \boldsymbol{\tau}_t \tag{21}$$

where $\boldsymbol{J}_t$ and $\boldsymbol{\omega}_t$ are the target's inertia matrix and angular velocity, and $\boldsymbol{\tau}_t$ is the external torque exerting on the target. According to the definition of the body fixed frame, the products of inertia in the frame F_T are zero. Therefore, in the frame F_T, the component form of (21) in the absence of torques is given as

$$\begin{cases} J_x \dot{\omega}_x + (J_z - J_y)\omega_z \omega_y = 0 \\ J_y \dot{\omega}_y + (J_x - J_z)\omega_x \omega_z = 0 \\ J_z \dot{\omega}_z + (J_y - J_x)\omega_y \omega_x = 0 \end{cases} \tag{22}$$

where ω_x, ω_y and ω_z are components of $\boldsymbol{\omega}_t$, and J_x, J_y and J_z are the target's principal moments of inertia. For simplicity, we make the realistic assumption that the target is an axially symmetric prolate rigid body [32], whose axis of symmetry of the inertia tensor is the axis x_t. With $J_x < J_y = J_z = J_{tr}$, (22) becomes

$$\begin{cases} \dot{\omega}_x = 0 \\ \dot{\omega}_y - (1 - J_x/J_{tr})\omega_x \omega_z = 0 \\ \dot{\omega}_z + (1 - J_x/J_{tr})\omega_x \omega_y = 0 \end{cases}. \tag{23}$$

The solution of (23) is

$$\begin{cases} \omega_x = \text{const} \\ \omega_y = \omega_{tr} \sin(\Omega_b t + \psi_0) \\ \omega_z = \omega_{tr} \cos(\Omega_b t + \psi_0) \end{cases} \tag{24}$$

where ω_{tr} is the transverse angular rate in the $y_t z_t$ plane, ψ_0 is a constant initial phase, and $\Omega_b = (1 - J_x/J_{tr})\omega_x$ is called the body nutation rate because it is the rate at which the angular velocity rotates about the symmetry axis in the body fixed frame.

The target's attitude kinematics are derived by employing 1-2-1 Euler angles (ϕ, θ, ψ). For convenience, suppose that axis x_I of the inertial reference frame F_I is parallel to the target's angular momentum vector $\boldsymbol{H}_t$ and we have

$$\dot{\phi} = \frac{H}{J_{tr}} = \Omega_s, \quad \dot{\theta} = 0, \quad \dot{\psi} = \Omega_b \tag{25}$$

where $H = \|\boldsymbol{H}_t\|$, Ω_s is called the inertial nutation rate because it is the rate at which $\boldsymbol{\omega}_t$ and the axis x_t rotate about the fixed angular momentum vector $\boldsymbol{H}_t$ in the frame F_I, and $\theta = \arccos(J_x \omega_x / H)$ is called the nutation angle which is the angle between $\boldsymbol{H}_t$ and the axis x_t. A pictorial view of the target's attitude motion is presented in Fig. 4.

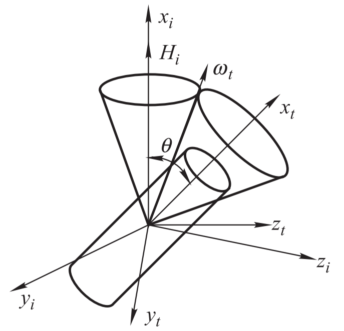

Fig. 4 Torque-free motion of an axially symmetric prolate rigid body

In practice, the attitude motion of the faulty spacecraft may be more complicated. However, limited by the maneuverability of real capturing mechanism, rendezvous will be carried out after conducting some detumbling operations [33–35]. Therefore, it is reasonable to represent the target's attitude motion by (23) and (25) in simulation analysis.

3.2 Dual-quaternion-based kinematics

Note that the superscript represents the frame in which a vector is expressed, while the subscript represents the object which a vector is related to.

The general motion of a rigid body is represented by the motion of its body fixed frame relative to the inertial reference frame. Suppose the position vector and attitude quaternion of the frame F_B with respect to the frame F_I are $\boldsymbol{r}$ and $\boldsymbol{q}$. Then the description of this spatial motion in terms of the dual quaternion is given as

$$\widehat{\boldsymbol{q}} = \boldsymbol{q} + \varepsilon\frac{1}{2}\boldsymbol{r}^i \circ \boldsymbol{q} = \boldsymbol{q} + \varepsilon\frac{1}{2}\boldsymbol{q} \circ \boldsymbol{r}^b. \tag{26}$$

Differentiating (26), the dual-quaternion-based kinematic equation of a single rigid body is given as

$$\dot{\widehat{\boldsymbol{q}}} = \frac{1}{2}\widehat{\boldsymbol{\omega}}^i \circ \widehat{\boldsymbol{q}} = \frac{1}{2}\widehat{\boldsymbol{q}} \circ \widehat{\boldsymbol{\omega}}^b \tag{27}$$

where $\widehat{\boldsymbol{\omega}}^i$ and $\widehat{\boldsymbol{\omega}}^b$ are velocity motors.

The relative motion between the chaser and the target is represented by the general motion of the frame F_C relative to the frame F_T. Since the difference between two dual quaternions is defined by multiplication, the error dual quaternion $\widehat{\boldsymbol{q}}_e$ is given as

$$\widehat{\boldsymbol{q}}_e = \widehat{\boldsymbol{q}}_t^* \circ \widehat{\boldsymbol{q}}_c = \boldsymbol{q}_e + \varepsilon\frac{1}{2}\boldsymbol{q}_e \circ (\boldsymbol{r}_c^c - \boldsymbol{q}_e^* \circ \boldsymbol{r}_t^t \circ \boldsymbol{q}_e) =$$

$$\boldsymbol{q}_e + \varepsilon\frac{1}{2}\boldsymbol{q}_e \circ \boldsymbol{r}_e^c = \boldsymbol{q}_e + \varepsilon\boldsymbol{q}_e' \tag{28}$$

where $\boldsymbol{q}_e = \boldsymbol{q}_t^* \circ \boldsymbol{q}_c$ is the attitude error quaternion, $\boldsymbol{r}_e^c = \boldsymbol{r}_c^c - \boldsymbol{q}_e^* \circ \boldsymbol{r}_t^t \circ \boldsymbol{q}_e$ is the positon vector of the frame F_C relative to the frame F_T.

Differentiating (28), the kinematic equation of relative motion between the chaser and the target can be given as

$$\dot{\widehat{\boldsymbol{q}}}_e = \dot{\widehat{\boldsymbol{q}}}_t^* \circ \widehat{\boldsymbol{q}}_c + \widehat{\boldsymbol{q}}_t^* \circ \dot{\widehat{\boldsymbol{q}}}_c =$$

$$\frac{1}{2}\widehat{\boldsymbol{q}}_e \circ (\widehat{\boldsymbol{\omega}}_c^c - \widehat{\boldsymbol{q}}_e^* \circ \widehat{\boldsymbol{\omega}}_t^t \circ \widehat{\boldsymbol{q}}_e) = \frac{1}{2}\widehat{\boldsymbol{q}}_e \circ \widehat{\boldsymbol{\omega}}_e^c \tag{29}$$

where $\widehat{\boldsymbol{\omega}}_e^c$ is the error velocity motor.

3.3 Dual-quaternion-based dynamics

To formulate the rigid body dynamic equation in the dual number form, we first define the dual inertia operator $\widehat{\boldsymbol{M}}$ as

$$\widehat{\boldsymbol{M}} = m\frac{\mathrm{d}}{\mathrm{d}\varepsilon}\boldsymbol{I} + \varepsilon\boldsymbol{J} \tag{30}$$

where m and $\boldsymbol{J}$ are the mass and the inertial matrix of the rigid body respectively. The operator $\mathrm{d}/\mathrm{d}\varepsilon$ has a complementary sense of the dual unit ε. By comparing operations of ε and $\mathrm{d}/\mathrm{d}\varepsilon$ on a dual vector $\widehat{\boldsymbol{a}}$, there is

$$\begin{cases} \varepsilon\widehat{\boldsymbol{a}} = \varepsilon(\boldsymbol{a} + \varepsilon\boldsymbol{a}') = \varepsilon\boldsymbol{a} \\ \dfrac{\mathrm{d}}{\mathrm{d}\varepsilon}\widehat{\boldsymbol{a}} = \dfrac{\mathrm{d}}{\mathrm{d}\varepsilon}(\boldsymbol{a} + \varepsilon\boldsymbol{a}') = \boldsymbol{a}' \end{cases}. \tag{31}$$

The inverse of $\widehat{\boldsymbol{M}}$ is defined as

$$\widehat{\boldsymbol{M}}^{-1} = \boldsymbol{J}^{-1}\frac{\mathrm{d}}{\mathrm{d}\varepsilon} + \varepsilon\frac{1}{m}\boldsymbol{I}. \tag{32}$$

The expression of the momentum motor $\widehat{\boldsymbol{H}}$ of a rigid body with respect to the c.m. can be written as

$$\widehat{\boldsymbol{H}} = \widehat{\boldsymbol{M}}\widehat{\boldsymbol{\omega}} = \left(m\frac{\mathrm{d}}{\mathrm{d}\varepsilon}\boldsymbol{I} + \varepsilon\boldsymbol{J}\right)(\boldsymbol{\omega} + \varepsilon\boldsymbol{v}) = m\boldsymbol{v} + \varepsilon\boldsymbol{J}\boldsymbol{\omega}. \tag{33}$$

Taking derivative of (33), the dual-quaternion-based dynamic equation of a single rigid body expressed in the frame F_B can be obtained as

$$\frac{\mathrm{d}\widehat{\boldsymbol{H}}^b}{\mathrm{d}t} = \widehat{\boldsymbol{M}}\dot{\widehat{\boldsymbol{\omega}}}^b + \widehat{\boldsymbol{\omega}}^b \times \widehat{\boldsymbol{M}}\widehat{\boldsymbol{\omega}}^b = \widehat{\boldsymbol{G}}^b + \widehat{\boldsymbol{U}}^b =$$

$$(\boldsymbol{G}^b + \varepsilon\boldsymbol{T}^b) + (\boldsymbol{f}^b + \varepsilon\boldsymbol{\tau}^b) \tag{34}$$

where $\widehat{\boldsymbol{G}}^b$ and $\widehat{\boldsymbol{U}}^b$ are the gravity motor and the control force motor, $\boldsymbol{G}^b = -\mu m\boldsymbol{r}^b/\|\boldsymbol{r}^b\|^3$ is the gravity, $\boldsymbol{T}^b = 3\mu\boldsymbol{r}^b \times (\boldsymbol{J} \cdot \boldsymbol{r}^b)/\|\boldsymbol{r}^b\|^5$ is the gravity gradient torque, and $\boldsymbol{f}^b$ and $\boldsymbol{\tau}^b$ are control force and torque respectively.

According to the definition of the error velocity motor, the chaser's velocity motor is written as

$$\widehat{\boldsymbol{\omega}}_c^c = \widehat{\boldsymbol{\omega}}_e^c + \widehat{\boldsymbol{q}}_e^* \circ \widehat{\boldsymbol{\omega}}_t^t \circ \widehat{\boldsymbol{q}}_e. \tag{35}$$

Substituting (35) into (34), there is

$$\frac{\mathrm{d}\boldsymbol{H}_c^c}{\mathrm{d}t} = \widehat{\boldsymbol{M}}_c \circ \frac{\mathrm{d}}{\mathrm{d}t}(\widehat{\boldsymbol{\omega}}_e^c + \widehat{\boldsymbol{q}}_e^* \circ \widehat{\boldsymbol{\omega}}_t^t \circ \widehat{\boldsymbol{q}}_e) + (\widehat{\boldsymbol{\omega}}_e^c + \widehat{\boldsymbol{q}}_e^* \circ \widehat{\boldsymbol{\omega}}_t^t \circ \widehat{\boldsymbol{q}}_e) \times$$

$$[\widehat{\boldsymbol{M}}_c \circ (\widehat{\boldsymbol{\omega}}_e^c + \widehat{\boldsymbol{q}}_e^* \circ \widehat{\boldsymbol{\omega}}_t^t \circ \widehat{\boldsymbol{q}}_e)] = (\boldsymbol{G}_c^c + \varepsilon\boldsymbol{T}_c^c) + (\boldsymbol{f}_c^c + \varepsilon\boldsymbol{\tau}_c^c). \tag{36}$$

After some manipulation of (36), the dynamic equation of relative motion expressed in the frame F_C is given as

$$\widehat{\boldsymbol{M}}_c\dot{\widehat{\boldsymbol{\omega}}}_e^c = -(\widehat{\boldsymbol{\omega}}_e^c + \widehat{\boldsymbol{q}}_e^* \circ \widehat{\boldsymbol{\omega}}_t^t \circ \widehat{\boldsymbol{q}}_e) \times [\widehat{\boldsymbol{M}}_c \circ (\widehat{\boldsymbol{\omega}}_e^c + \widehat{\boldsymbol{q}}_e^* \circ \widehat{\boldsymbol{\omega}}_t^t \circ \widehat{\boldsymbol{q}}_e)] - \widehat{\boldsymbol{M}}_c[\widehat{\boldsymbol{q}}_e^* \circ \dot{\widehat{\boldsymbol{\omega}}}_t^t \circ \widehat{\boldsymbol{q}}_e - \widehat{\boldsymbol{\omega}}_e^c \times (\widehat{\boldsymbol{q}}_e^* \circ \widehat{\boldsymbol{\omega}}_t^t \circ \widehat{\boldsymbol{q}}_e)] + \widehat{\boldsymbol{G}}_c^c + \boldsymbol{U}_c^c. \tag{37}$$

Let $\boldsymbol{F}(\widehat{\boldsymbol{\omega}}_e^c, \widehat{\boldsymbol{q}}_e) = -(\widehat{\boldsymbol{\omega}}_e^c + \widehat{\boldsymbol{q}}_e^* \circ \widehat{\boldsymbol{\omega}}_t^t \circ \widehat{\boldsymbol{q}}_e) \times [\widehat{\boldsymbol{M}}_c \circ (\widehat{\boldsymbol{\omega}}_e^c + (\widehat{\boldsymbol{q}}_e^* \circ \widehat{\boldsymbol{\omega}}_t^t \circ \widehat{\boldsymbol{q}}_e)] - \widehat{\boldsymbol{M}}_c[\widehat{\boldsymbol{q}}_e^* \circ \dot{\widehat{\boldsymbol{\omega}}}_t^t \circ \widehat{\boldsymbol{q}}_e - \widehat{\boldsymbol{\omega}}_e^c \times (\widehat{\boldsymbol{q}}_e^* \circ \widehat{\boldsymbol{\omega}}_t^t \circ \widehat{\boldsymbol{q}}_e)] + \widehat{\boldsymbol{G}}_c^c$, then a more compact form of (37) can be given as

$$\widehat{\boldsymbol{M}}_c\dot{\widehat{\boldsymbol{\omega}}}_e^c = \boldsymbol{F}(\widehat{\boldsymbol{\omega}}_e^c, \widehat{\boldsymbol{q}}_e) + \boldsymbol{U}_c^c. \tag{38}$$

3.4 Effects of the target attitude motion

The dual-quaternion-based model of the 6-DOF relative motion is represented by (29) and (37). To facilitate the subsequent analysis and design, the integrated model is decomposed into real and dual parts. For brevity, the following definitions are given as

$$\begin{cases} \widehat{\boldsymbol{\omega}}_e^c = \boldsymbol{\omega}_e^c + \varepsilon \boldsymbol{v}_e^c \\ \widehat{\boldsymbol{\omega}}_t^t = \boldsymbol{\omega}_t^t + \varepsilon \boldsymbol{v}_t^t \end{cases}. \tag{39}$$

Then the decomposition form of the error kinematic equation (29) can be written as

$$\begin{cases} \dot{\boldsymbol{q}}_e = \dfrac{1}{2}\boldsymbol{q}_e \circ \boldsymbol{\omega}_e^c \\ \dot{\boldsymbol{q}}_e' = \dfrac{1}{2}(\boldsymbol{q}_e' \circ \boldsymbol{\omega}_e^c + \boldsymbol{q}_e \circ \boldsymbol{v}_e^c) \end{cases}. \tag{40}$$

The decomposition form of the error dynamic equation (37) is given as

$$\begin{aligned} \dot{\boldsymbol{\omega}}_e^c &= -\boldsymbol{J}_c^{-1}[(\boldsymbol{\omega}_e^c + \boldsymbol{C}_{ct}\boldsymbol{\omega}_t^t) \times \boldsymbol{J}(\boldsymbol{\omega}_e^c + \boldsymbol{C}_{ct}\boldsymbol{\omega}_t^t)] - \boldsymbol{C}_{ct}\dot{\boldsymbol{\omega}}_t^t - \boldsymbol{C}_{ct}\boldsymbol{\omega}_t^t \times \boldsymbol{\omega}_e^c + \boldsymbol{J}_c^{-1}\frac{3\mu}{r_c^5}\boldsymbol{r}_c^c \times (\boldsymbol{J}_c \cdot \boldsymbol{r}_c^c) + \boldsymbol{J}_c^{-1}\boldsymbol{\tau}_c^c \\ \dot{\boldsymbol{v}}_e^c &= -2\boldsymbol{C}_{ct}\boldsymbol{\omega}_t^t \times \boldsymbol{v}_e^c - \boldsymbol{C}_{ct}\boldsymbol{\omega}_t^t \times (\boldsymbol{C}_{ct}\boldsymbol{v}_t^t + \boldsymbol{C}_{ct}\boldsymbol{\omega}_t^t \times \boldsymbol{r}_e^c) - \boldsymbol{\omega}_e^c \times \boldsymbol{v}_e^c + \boldsymbol{C}_{ct}(\boldsymbol{\omega}_t^t \times \boldsymbol{v}_t^t) + \frac{\mu}{r_t^3}\boldsymbol{C}_{ct}\boldsymbol{r}_t^t + \frac{1}{m_c}\left(\boldsymbol{f}_c^c - \frac{\mu m_c}{r_c^3}\boldsymbol{r}_c^c\right) \end{aligned} \tag{41}$$

where r_c and r_t are the orbit radius, $\boldsymbol{C}_{ct} = \boldsymbol{C}(\boldsymbol{q}_e)$ is the DCM which transforms coordinates in the frame F_T to the frame F_C. Since the distance between the chaser and the target is negligible compared to the orbit radius, r_c and r_t are considered to be equal, and orbit frames of the chaser and the target are also regarded as the same.

The model of relative motion given in [17] is derived based on a key assumption that the target's body fixed frame is always aligned with its orbit frame. Therefore, the expressions of radius, linear and angular velocity vectors in the frame F_B are the same as those in the frame F_O and are fixed, namely,

$$\begin{cases} \boldsymbol{r}_t^t = \boldsymbol{r}_t^o = [0 \quad 0 \quad -r_t]^{\mathrm{T}} \\ \boldsymbol{r}_c^c = \boldsymbol{r}_c^o = [0 \quad 0 \quad -r_c]^{\mathrm{T}} \\ \boldsymbol{v}_t^t = \boldsymbol{v}_t^o = [v_t \quad 0 \quad 0]^{\mathrm{T}} \\ \boldsymbol{\omega}_t^t = \boldsymbol{\omega}_t^o = [0 \quad -\omega_t \quad 0]^{\mathrm{T}} \end{cases} \tag{42}$$

Due to the target's attitude motion, this assumption cannot hold anymore. However, if the transformation relationships between two body fixed frames and the orbit frame are known, their expressions in the frame F_B can be converted from those in the frame F_O.

The target's angular velocity expressed in the frame F_T is directly given in (24) when deriving attitude dynamics of the target in Section 3.1.

Based on attitude kinematics of the target, the DCM $\boldsymbol{C}_{ti}$ that transforms coordinates in the frame F_I to the frame F_T can be calculated. According to the chaser's orbit elements, the DCM $\boldsymbol{C}_{oi}$ that transforms coordinates in the frame F_I to the frame F_O can be calculated. Consequently, we have the following relationships between the orbit frame and body fixed frames:

$$\begin{cases} \boldsymbol{C}_{to} = \boldsymbol{C}_{ti}\boldsymbol{C}_{io} \\ \boldsymbol{C}_{co} = \boldsymbol{C}_{ct}\boldsymbol{C}_{to} \end{cases} \tag{43}$$

where $\boldsymbol{C}_{to}$ transforms coordinates in the frame F_O to the frame F_T, $\boldsymbol{C}_{co}$ transforms coordinates in the frame F_O to the frame F_C.

Therefore, the radius and linear velocity vectors expressed in body fixed frames can be calculated as

$$\begin{cases} \boldsymbol{r}_t^t = \boldsymbol{C}_{to}\boldsymbol{r}_t^o \\ \boldsymbol{r}_c^c = \boldsymbol{C}_{co}\boldsymbol{r}_c^o \\ \boldsymbol{v}_t^t = \boldsymbol{C}_{to}\boldsymbol{v}_t^o \end{cases}. \tag{44}$$

Substituting (42) with (24) and (44), we can obtain the model of relative motion between the chaser and a tumbling target.

3.5 Control law design

In this section, we deal with the 6-DOF tracking control problem of the chaser relative to a tumbling target. Since the attitude of the target is time-varying, the objective of tracking control is to design a controller that enables the chaser to be synchronous with the attitude of the target and to approach the target from the initial position to the desired berth point which has a safe distance of 2 m to the target.

To guarantee the system converge to the desired state fast and steadily, and to have high control precision in the presence external disturbances, a sliding mode controller based on the exponential reaching law and the continuous relay function is designed.

To begin with, define the linear sliding surface as

$$\widehat{\boldsymbol{s}} = \boldsymbol{s} + \varepsilon \boldsymbol{s}' = \widehat{\boldsymbol{\omega}}_e^c + \widehat{\boldsymbol{c}} \otimes \widehat{\boldsymbol{e}} \tag{45}$$

where $\widehat{\boldsymbol{c}} = \boldsymbol{c} + \varepsilon \boldsymbol{c}'$ is a parameter of the linear sliding surface and its components are positive real numbers, $\widehat{\boldsymbol{e}} = \boldsymbol{e} + \varepsilon \boldsymbol{e}' = 2 \ln \widehat{\boldsymbol{q}}_e$ represents the error of relative attitude and position. According to (9) and (20), we have $\widehat{\boldsymbol{e}} = \varPhi_e \boldsymbol{q}_{ev} + \varepsilon \boldsymbol{r}_e^c$.

Consider two dual quaternions $\widehat{\boldsymbol{a}} = \boldsymbol{a} + \varepsilon \boldsymbol{a}'$ and $\widehat{\boldsymbol{b}} = \boldsymbol{b} + \varepsilon \boldsymbol{b}'$, then operation '$\otimes$' written in the vector form is defined as

$$\widehat{\boldsymbol{a}} \otimes \widehat{\boldsymbol{b}} = \begin{bmatrix} D(\boldsymbol{a})\boldsymbol{b} \\ D(\boldsymbol{a}')\boldsymbol{b}' \end{bmatrix} \tag{46}$$

where $D(\boldsymbol{a})$ is defined as

$$D(\boldsymbol{a}) = \operatorname{diag}(\boldsymbol{a}). \tag{47}$$

According to the exponential reaching law, there is

$$\dot{\widehat{\boldsymbol{s}}} = -\widehat{\boldsymbol{\delta}} \otimes \theta(\widehat{\boldsymbol{s}}) - \widehat{\boldsymbol{k}} \otimes \widehat{\boldsymbol{s}} \tag{48}$$

where $\widehat{\boldsymbol{\delta}} = \boldsymbol{\delta} + \varepsilon \boldsymbol{\delta}'$ and $\widehat{\boldsymbol{k}} = \boldsymbol{k} + \varepsilon \boldsymbol{k}'$ are parameters, all of whose components are positive real numbers. $\theta(\widehat{\boldsymbol{s}})$ is a continuous relay function and is given as

$$\theta(s_i) = s_i/(|s_i| + \sigma_i), \quad i = 1, 2, \ldots, 6 \tag{49}$$

where σ_i is a small positive real number.

The controller is designed as

$$\begin{aligned} \widehat{\boldsymbol{U}}_c^c = -\boldsymbol{F}(\widehat{\boldsymbol{\omega}}_e^c, \widehat{\boldsymbol{q}}_e) - \widehat{\boldsymbol{M}}_c(\widehat{\boldsymbol{c}} \otimes \dot{\widehat{\boldsymbol{e}}}) - \\ \widehat{\boldsymbol{\delta}} \otimes \theta(\widehat{\boldsymbol{s}}^s) - \widehat{\boldsymbol{k}} \otimes \widehat{\boldsymbol{s}}^s \end{aligned} \tag{50}$$

where $\dot{\widehat{\boldsymbol{e}}} = \dot{\boldsymbol{e}} + \varepsilon \dot{\boldsymbol{e}}'$ is calculated [17] as

$$\begin{cases} \dot{\boldsymbol{e}} = \boldsymbol{\omega}_e^c + \dfrac{1}{2}\boldsymbol{e} \times \boldsymbol{\omega}_e^c + \dfrac{2 - \varPhi_e \cot(\varPhi_e/2)}{2\varPhi_e^2}\boldsymbol{\omega}_e^c \times \\ \quad (\boldsymbol{e} \times \boldsymbol{\omega}_e^c) \\ \dot{\boldsymbol{e}}' = \boldsymbol{v}_e^c - \boldsymbol{\omega}_e^c \times \boldsymbol{r}_e^c \boldsymbol{e}' \end{cases}. \tag{51}$$

The stability of the resultant closed-loop system is stated in the following theorem.

Theorem 1 Consider the 6-DOF tracking system given by (30) and (38). By employing the controller (48), $(\widehat{\boldsymbol{e}}, \widehat{\boldsymbol{\omega}}_{\boldsymbol{e}}^{\boldsymbol{c}}) \to (\widehat{\boldsymbol{0}}, \widehat{\boldsymbol{0}})$ as $t \to \infty$ for all initial conditions.

Proof The proof includes the following two consecutive steps:

(i) The closed-loop system can reach the sliding surface $\widehat{\boldsymbol{s}} = \widehat{\boldsymbol{0}}$ for all initial conditions.

(ii) After reaching $\widehat{\boldsymbol{s}} = \widehat{\boldsymbol{0}}$, the tracking error $(\widehat{\boldsymbol{e}}, \widehat{\boldsymbol{\omega}}_{\boldsymbol{e}}^{\boldsymbol{c}}) \to (\widehat{\boldsymbol{0}}, \widehat{\boldsymbol{0}})$ as $t \to \infty$.

The first Lyapunov function is chosen as

$$V_1 = \frac{1}{2}\widehat{\boldsymbol{s}}^s \odot (\widehat{\boldsymbol{M}}_c \widehat{\boldsymbol{s}}). \tag{52}$$

According to the definitions of the circle product and the swap given in (16), we have

$$V_1 = \frac{1}{2}\widehat{\boldsymbol{s}}^s \odot (\widehat{\boldsymbol{M}}_c \widehat{\boldsymbol{s}}) = \frac{1}{2}(m\boldsymbol{s}' \cdot \boldsymbol{s}' + \boldsymbol{s} \cdot \boldsymbol{J}\boldsymbol{s}). \tag{53}$$

Note that V_1 is a valid Lyapunov function, since $V_1 \geqslant 0$ and $V_1 = 0$ if and only if $\widehat{\boldsymbol{s}} = \widehat{\boldsymbol{0}}$. The derivative of (49) is given as

$$\begin{aligned} \dot{V}_1 = \widehat{\boldsymbol{s}}^s \odot (\widehat{\boldsymbol{M}}_c \dot{\widehat{\boldsymbol{s}}}) = \\ \widehat{\boldsymbol{s}}^s \odot (\boldsymbol{U}_c^c + \boldsymbol{F}(\widehat{\boldsymbol{\omega}}_e^c, \widehat{\boldsymbol{q}}_e) + \widehat{\boldsymbol{M}}_c(\widehat{\boldsymbol{c}} \otimes \dot{\widehat{\boldsymbol{e}}}_e^c)). \end{aligned} \tag{54}$$

Substituting the control law (49) into (52), there is

$$\begin{aligned} \dot{V}_1 = \widehat{\boldsymbol{s}}^s \odot (-\widehat{\boldsymbol{\delta}} \otimes \theta(\widehat{\boldsymbol{s}}^s) - \widehat{\boldsymbol{k}} \otimes \widehat{\boldsymbol{s}}^s) = \\ -\boldsymbol{s}' \cdot (D(\boldsymbol{\delta})\theta(\boldsymbol{s}') + D(\boldsymbol{k})\boldsymbol{s}') - \\ \boldsymbol{s} \cdot (D(\boldsymbol{\delta}')\theta(\boldsymbol{s}) + D(\boldsymbol{k}')\boldsymbol{s}). \end{aligned} \tag{55}$$

Since $D(\boldsymbol{\delta})$, $D(\boldsymbol{\delta}')$, $D(\boldsymbol{k})$ and $D(\boldsymbol{k}')$ are positive matrices, $\dot{V}_1 \leqslant 0$. If and only if $\widehat{\boldsymbol{s}} = \widehat{\boldsymbol{0}}$, there is $\dot{V}_1 = 0$. Hence the closed-loop system can reach the sliding surface $\widehat{\boldsymbol{s}} = \widehat{\boldsymbol{0}}$ for all initial conditions.

Since $V_1 \geqslant 0$ and $\dot{V}_1 \leqslant 0$, $\lim\limits_{t\to\infty} V_1(t)$ exists and is finite. Hence

$$\lim_{t\to\infty} \int_0^t \dot{V}_1(\tau)\mathrm{d}\tau = \lim_{t\to\infty} V_1(t) - V_1(0) \tag{56}$$

also exists and is finite. By Barbalat's lemma, $\lim\limits_{t\to\infty} V_1(t) = 0$ and thus $\lim\limits_{t\to\infty} \widehat{\boldsymbol{s}}(t) = \widehat{\boldsymbol{0}}$.

After reaching $\widehat{\boldsymbol{s}} = \widehat{\boldsymbol{0}}$, we have

$$\widehat{\boldsymbol{\omega}}_e^c = -\widehat{\boldsymbol{c}} \otimes \widehat{\boldsymbol{e}}. \tag{57}$$

Then consider the following Lyapunov function

$$V_2 = \frac{1}{2}\widehat{\boldsymbol{e}} \odot \widehat{\boldsymbol{e}} \geqslant 0. \tag{58}$$

$V_2 = 0$ if and only if $\widehat{\boldsymbol{e}} = \widehat{\boldsymbol{0}}$. According to (51) and (56), the derivative of (49) is calculated as

$$\begin{aligned} \dot{V}_2 = \widehat{\boldsymbol{e}} \odot \dot{\widehat{\boldsymbol{e}}} = \boldsymbol{e} \cdot \boldsymbol{\omega}_e^c + \boldsymbol{e}'\boldsymbol{v}_e^c = \\ -\boldsymbol{e} \cdot (D(\boldsymbol{c})\boldsymbol{e}) - \boldsymbol{e}' \cdot (D(\boldsymbol{c}')\boldsymbol{e}'). \end{aligned} \tag{59}$$

$D(\boldsymbol{c})$ and $D(\boldsymbol{c}')$ are positive matrices, so $\dot{V}_2 \leqslant 0$. Since $V_2 \geqslant 0$ and $\dot{V}_2 \leqslant 0$, $\lim\limits_{t\to\infty} V_2(t)$ exists and is finite. Hence

$$\lim_{t\to\infty} \int_0^t \dot{V}_2(\tau)\mathrm{d}\tau = \lim_{t\to\infty} V_2(t) - V_2(0) \tag{60}$$

also exists and is finite. It then follows from Barbalat's lemma that $\lim\limits_{t\to\infty} \widehat{\boldsymbol{e}}(t) = \widehat{\boldsymbol{0}}$. Along with $\lim\limits_{t\to\infty} \widehat{\boldsymbol{s}}(t) = \widehat{\boldsymbol{\omega}}_e^c + \widehat{\boldsymbol{c}} \otimes \widehat{\boldsymbol{e}} = \widehat{\boldsymbol{0}}$, there is $\lim\limits_{t\to\infty} \widehat{\boldsymbol{\omega}}_e^c(t) = \widehat{\boldsymbol{0}}$. □

4. Simulation analysis

In this section, the control law (40) are numerically simulated. Under the same initial conditions, its anti-interference ability is compared with the generalized proportional differential controller designed in [36].

The target inertial matrix is $\boldsymbol{J}_t = \mathrm{diag}[300, 800, 800]\ \mathrm{kg\cdot m^2}$. It is assumed to be an uncontrolled satellite in geosynchronous orbit with the torque-free attitude motion. Its spin angular rate is $\omega_x = 8\ {}^\circ/\mathrm{s}$ and the nutation angle is $\theta = 3^\circ$. According to Section 3.1, the attitude motion of the target can be calculated as

$$\begin{cases} \boldsymbol{\omega}_t^t = [8 \quad 0.16\sin(5t) \quad 0.16\cos(5t)]^{\mathrm{T}} \\ [\phi \quad \theta \quad \psi]^{\mathrm{T}} = [3t \quad 3 \quad 5t]^{\mathrm{T}} \end{cases}. \tag{61}$$

The chaser's inertia matrix and mass are $\boldsymbol{J}_c = \mathrm{diag}[450, 1\,625, 1\,625]\ \mathrm{kg\cdot m^2}$ and $m_c = 1\,000\ \mathrm{kg}$. It orbits the earth in approximately geosynchronous orbit. Its argument of perigee is 221.32°, right ascension of the ascending node is 85.24°, and initial true anomaly is 111.66°. The initial parameters of the relative motion are given as

$$\begin{cases} \widehat{\boldsymbol{q}}_{e0} = \boldsymbol{q}_{e0} + \varepsilon \dfrac{1}{2} \boldsymbol{q}_{e0} \circ \boldsymbol{r}_{e0}^c \\ \widehat{\boldsymbol{\omega}}_{e0}^c = \boldsymbol{\omega}_{e0}^c + (\dot{\boldsymbol{r}}_{e0}^c + \boldsymbol{\omega}_{e0}^c \times \boldsymbol{r}_{e0}^c) \end{cases} \tag{62}$$

where $\boldsymbol{r}_{e0}^c = [-20 \quad 8 \quad 6]^{\mathrm{T}}$ m, $\boldsymbol{q}_{e0} = [0.554 \quad 0.791 \quad -0.226 \quad 0.258]^{\mathrm{T}}$, $\dot{\boldsymbol{r}}_{e0}^c = [0 \quad 0 \quad 0]^{\mathrm{T}}$, $\boldsymbol{\omega}_{e0}^c = -[0.14 \quad 0.002 \quad 0.001]^{\mathrm{T}}$.

The disturbance torque and force acting on the chaser are set as

$$\begin{cases} \boldsymbol{\tau}_d^c = [0.13 \quad 0.13 \quad 0.13]^{\mathrm{T}} + N(0, v) \\ \boldsymbol{f}_d^c = [0.22 \quad 0.22 \quad 0.22]^{\mathrm{T}} + N(0, v) \end{cases} \tag{63}$$

where $N(0, v)$ is white Gaussian noise with zero mean value and variance $v = 1 \times 10^{-4}$.

To be intuitionistic, the relative rotation and translation errors are represented by 3-2-1 Euler angles and relative position, whose time histories are given in Fig. 5 and Fig. 6.

Time histories of relative linear and angular velocities are given in Fig. 7 and Fig. 8. It can be seen that relative rotation and translation converge to the desired state steadily. Fig. 9 and Fig. 10 give the time responses of control torque and force.

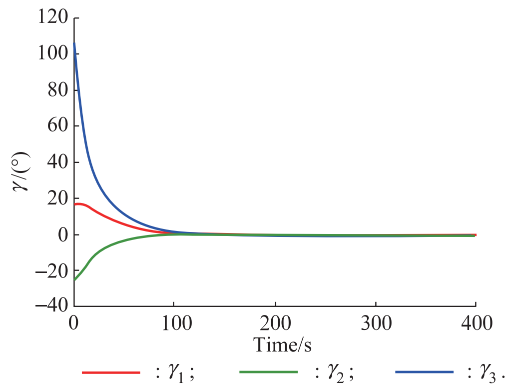

Fig. 5 Relative attitude angle

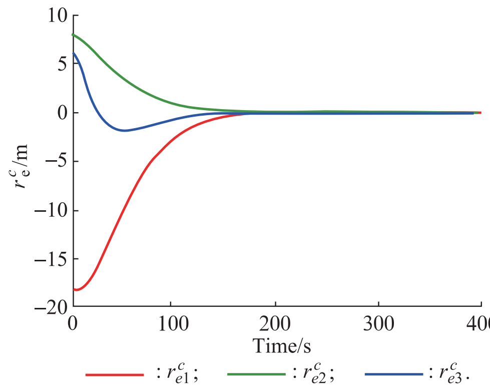

Fig. 6 Relative position

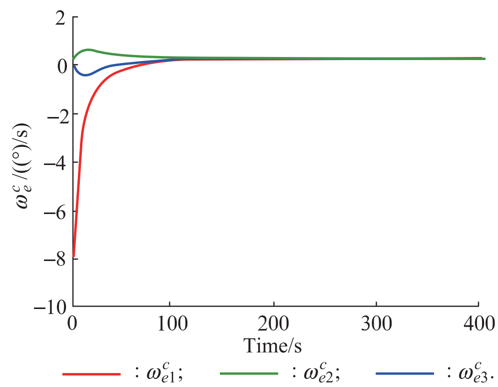

Fig. 7 Relative angle velocity

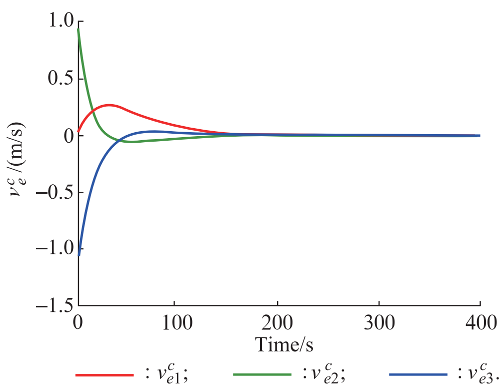

Fig. 8 Relative linear velocity

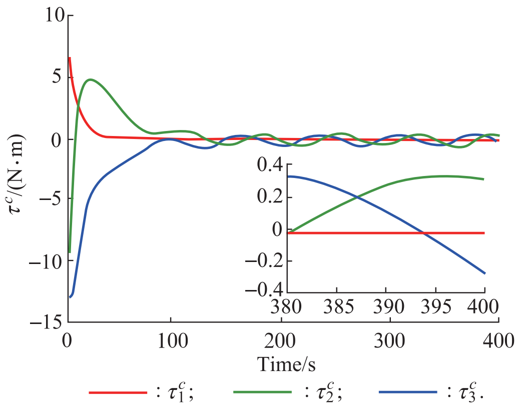

Fig. 9 Control torque

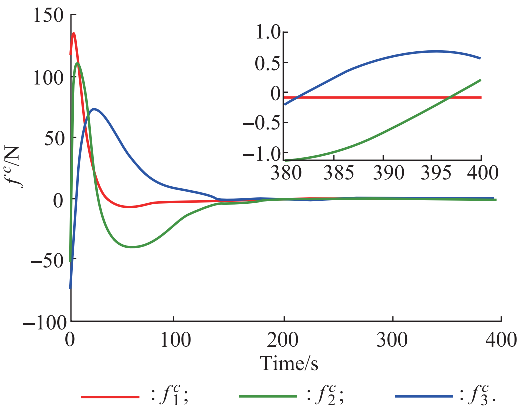

Fig. 10 Control force

The control precision is represented by the error values at the end of the control process, as shown in Table 1. It can be seen that the control force and torque are smooth and have little chattering. The relative attitude and position errors are within 0.05° and 1 mm at time of 400 s, which indicate the controller can achieve high control precision.

Table 1 Control results at time of 400 s

State variable	Value
Relative attitude/(°)	$10^{-2}\times[4.80\quad 4.79\quad 4.80]^{\mathrm{T}}$
Relative position/m	$10^{-4}\times[8.71\quad 5.67\quad 9.82]^{\mathrm{T}}$

The anti-interference capacity of the controller (50) is compared with that of the generalized PD controller in [36], whose control parameters are tuned so that the settling time and control precision are similar to those of the controller (50). The simulation results show that to achieve the same control precision, the magnitudes of the disturbance torque and force that the PD controller can withstand are $\tau_{d,PD}^c = 0.18\boldsymbol{\tau}_d^c$ and $\boldsymbol{f}_{d,PD}^c = 0.004\boldsymbol{f}_d^c$, which are much smaller.

5. Conclusions

In this paper, the integrated model of the coupled relative rotational and translational motion between a chaser and an uncontrolled tumbling target is developed by using the dual quaternion representation. For the short period of the final approaching phrase, the target's attitude motion is described by the torque-free motion of a prolate rigid body. After deriving the relative dynamics in the chaser's body fixed frame, this integrated model is decomposed into two parts. The decomposition form indicates the coupling terms clearly and shows the influence of the target's attitude motion on the descriptions of some important physical quantities in the model, which are then modified. A sliding mode controller based on the exponential reaching law and the continuous relay function is designed to guarantee synchronization control of the 6-DOF relative motion in the presence of external disturbances. The simulations results show the proposed controller is effective and of high accuracy. The new model given provides the foundation for further research. In future work, more control algorithms can be developed to improve the performance of motion tracking of the tumbling target.

References

[1] SHAN M H, GUO J, GILL E. Review and comparison of active space debris capturing and removal methods. Progress in Aerospace Sciences, 2016, 80: 18 – 32.

[2] ABAD A F, MA O, PHAM K, et al. A review of space robotics technologies for on-orbit servicing. Progress in Aerospace Sciences, 2014, 68: 1 – 26.

[3] GOMEZ N O, WALKER S J I. Earth's gravity gradient and eddy currents effects on the rotational dynamics of space debris objects: envisat case study. Advances in Space Research, 2015, 56(3): 494 – 508.

[4] PRALY N, HILLION M, BONNAL J, et al. Study on the eddy current damping of the spin dynamics of space debris from the Ariane launcher upper stages. Acta Astronautica, 2012, 76(4): 145 – 153.

[5] GURFIL P. Relative motion between elliptic orbits: generalized boundedness conditions and optimal formation keeping. Journal of Guidance, Control, and Dynamics, 2005, 28(4): 761 – 767.

[6] SABOL C, BURNS R, MCLAUGHLIN C A. Satellite formation flying design and evolution. Journal of Spacecraft and Rockets, 2001, 38(2): 270 – 278.

[7] MISHNE D. Formation control of satellites subject to drag variations and J2 perturbations. Journal of Guidance, Control, and Dynamics, 2004, 27(4): 685 – 692.

[8] SEGAL S, GURFIL P. Effect of kinematic rotation-translation coupling on relative spacecraft translational dynamics. Journal of Guidance, Control, and Dynamics, 2009, 32(3): 1045 – 1050.

[9] LI Q, YUAN J P, ZHANG B, et al. Model predictive control for autonomous rendezvous and docking with a tumbling target. Aerospace Science and Technology, 2017, 69: 700 – 711.

[10] JIANG B Y, HU Q L, FISHWELL M I. Fixed-time rendezvous control of spacecraft with a tumbling target under loss of actuator effectiveness. IEEE Trans. on Aerospace and Electronic Systems, 2016, 52(4): 1576 – 1586.

[11] WANG X L, ZHOU Z C, HU G J. Global fast terminal sliding mode control of space manipulator for capturing a tumbling satellite. Proc. of the 2nd IEEE Advanced Information Technology Electronic and Automation Control Conference, 2017: 553 – 558.

[12] CHEN B L, GENG Y H. Super twisting controller for on-orbit servicing to noncooperative target. Chinese Journal of Aeronautics, 2015, 28(1): 285 – 293.

[13] ZHANG D Y, LUO J J, GAO D W, et al. A novel nonlinear control for tracking and rendezvous with a rotating noncooperative target with translational maneuver. Acta Astronautica, 2017, 138: 279 – 289

[14] FUNDA J, RICHARD P P. A computational analysis of screw transformations in robotics. IEEE Trans. on Robotics and Automation, 1990, 6(3): 348 – 356.

[15] WU Y X, HU X P, HU D W, et al. Strapdown inertial navigation system algorithms based on dual quaternions. IEEE Trans. on Aerospace Electronic Systems, 2005, 41(1): 110 – 132.

[16] THOMAS F. Approaching dual quaternions from matrix algebra. IEEE Trans. on Robotics, 2014, 30(5): 1037 – 1048.

[17] SHARKAWY A N, ASRAGATHOS N. A comparative study of two methods for forward kinematics and Jacobian matrix determination. Proc. of the International Conference on Mechanical, System and Control Engineering, 2017: 179 – 183.

[18] BRODSKY V, SHOHAM M. Dual numbers representation of rigid body dynamics. Mechanism and Machine Theory, 1999, 34(5): 693 – 718.

[19] WANG J Y, LIANG H C, SUN Z W, et al. Finite-time control for spacecraft formation with dual-number-based description. Journal of Guidance, Control, and Dynamics, 2012, 35(3): 950 – 962.

[20] DONG H Y, HU Q L, MA G F. Dual-quaternion based fault-tolerant control for spacecraft formation flying with finite-time convergence. ISA Transactions, 2016, 61(99): 87 – 94.

[21] FILIPE N, TSIOTRAS P. Adaptive position and attitude-tracking controller for satellite proximity operations using dual quaternions. Journal of Guidance, Control, and Dynamics, 2015, 38(4): 566 – 577.

[22] GUI H C, VUKOVICH G. Dual quaternion based adaptive motion tracking of spacecraft with reduced control effort. Nonlinear Dynamics, 2016, 83(1/2): 597 – 614.

[23] GAO W, ZHU X G, ZHOU M L, et al. ADRC law of spacecraft rendezvous and docking in final approach phase. Journal of Cybernetics, 2016, 47(3): 236 – 248.

[24] KAZEMIPOUR A, NOVINZADEH A B. Adaptive position and attitude tracking control for satellite proximity operations using sliding mode and time delay estimation. Proc. of the 25th Iranian Conference on Electrical, 2017: 585 – 590.

[25] DONG H Y, HU Q L, AKELLA M R. Dual-quaternion-based spacecraft autonomous rendezvous and docking under six-degree-of-freedom motion constraints. Journal of Guidance, Control, and Dynamics, 2018, 41(5): 1150 – 1162.

[26] LU W, GENG Y H, CHEN X Q, et al. Relative position and attitude coupled control for autonomous docking with a tumbling target. International Journal of Control and Automation, 2011, 4(4): 1 – 22.

[27] CHEN B L, GENG Y H. Super twisting controller for on-orbit servicing to noncooperative target. Chinese Journal of Aeronautics, 2015, 28(1): 285 – 293.

[28] BRODSKY V, SHOHAM M. Dual numbers representation of rigid body dynamics. Mechanism and Machine Theory, 1999, 34(5): 693 – 718.

[29] WANG J Y, LIANG H C, SUN Z W, et al. Relative motion coupled control based on dual quaternion. Aerospace Science Technology, 2013, 25(1): 102 – 113.

[30] COHEN A, SHOHAM M. Principle of transference — an extension to hyper — dual numbers. Mechanism and Machine Theory, 2018, 125(1): 101 – 110.

[31] KUSSABA H T M, FIGUEREDO L F C, ISHIHARA J Y, et al. Hybrid kinematic control for rigid body pose stabilization using dual quaternions. Journal of the Franklin Institute, 2017, 354(7): 2769 – 2787.

[32] MARKLEY F L, CRASSIDIS J L. Fundamentals of spacecraft attitude determination and control. New York: Springer, 2014.

[33] NAKAJIMA Y, MITANI S, TANI H, et al. Detumbling space debris via thruster plume impingement. Proc. of the AIAA/AAS Astrodynamics Dynamics Specialist Conference, 2016: 5660 – 5679.

[34] YOUNGQUIST R C, NURGE M A, STARR S, et al. A slowly rotating hollow sphere in a magnetic field: first steps to de-spin a space object. American Journal of Physics, 2016, 84(3): 181 – 191.

[35] GOMEZ N O, WALKER S J I. Eddy currents applied to detumbling of space debris: analysis and validation of approximate proposed methods. Acta Astronautica, 2015, 114: 34 – 53.

[36] PENG X, SHI X P, GONG Y P. Integrated modeling of spacecraft relative motion dynamics using dual quaternion. Journal of Systems Engineering and Electronics, 2018, 29(2): 367 – 377.

Biographies

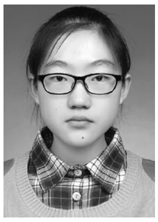

PENG Xuan was born in 1993. She received her B.S. degree in automation from Harbin Institute of Technology in 2016. She is currently a Ph.D. candidate in Harbin Institute of Technology. Her research interests are dual quaternion, attitude and orbit coupled control of spacecraft.
E-mail: 18745047873@163.com

SHI Xiaoping was born in 1965. He received his Ph.D. degree in spacecraft navigation guidance and control from Harbin Institute of Technology in 1994. He is currently a professor at the Control and Simulation Center, Harbin Institute of Technology. His research interests are aircraft control, nonlinear control, and complex system simulation.
E-mail: sxp@hit.edu.cn

GONG Yupeng was born in 1993. He received his B.S. degree in spacecraft design and engineering from Harbin Institute of Technology in 2015. He is currently a Ph.D. candidate in Harbin Institute of Technology. His research interests are orbital dynamics of satellite swarms and design of satellite constellation.
E-mail: GTYPHIT@163.com